SOME EXTENSIONS OF LOG AESTHETIC CURVES AND ITS ACCELERATION USING GENERAL PROCESSING UNIT (GPU)

TEH YEE MENG

UNIVERSITI SAINS MALAYSIA

2022

SOME EXTENSIONS OF LOG AESTHETIC CURVES AND ITS ACCELERATION USING GENERAL PROCESSING UNIT (GPU)

by

TEH YEE MENG

**Thesis submitted in fulfilment of the requirements
for the degree of
Doctor of Philosophy**

October 2022

ACKNOWLEDGEMENT

TABLE OF CONTENTS

LIST OF TABLES

LIST OF FIGURES

LIST OF ABBREVIATIONS

CAD	Computer Aided Design
CAGD	Computer Aided Geometric Design
CB	Coon's Bézier
CPU	Central Processing Unit
CUDA	Compute Unified Device Architecture
DP	Dormand-Prince
GK	Garisan Kelengkungan
GPU	General Processing Unit
IVP	Initial Value Problem
LAC	Logarithmic Aesthetic Curve
LA	Log Aesthetic
LASC	Log Aesthetic Space Curve
LCG	Logarithmic Curvature Graph
LDDC	Logarithmic Distribution Diagram of Curvature
LE	Log Estetik
LLE	Lengkung Log Estetik
LoC	Line of Curvature
LRLE	Lengkung Ruang Log Estetik
ODE	Ordinary Differential Equation
QB	Quadratic Bézier
RK	Runge-Kutta
RK4	Classical Runge-Kutta

LIST OF APPENDICES

x

BEBERAPA PERLUASAN LENGKUNG LOG ESTETIK DAN

KEPANTASANNYA DENGAN PENGGUNAAN UNIT PEMPROSESAN AM

ABSTRAK

Bahagian pertama adalah menyiasat ciri-ciri Lengkung Log Estetik (LLE) secara terperinci. Bahagian kedua mencadangkan teknik baru untuk mempercepatkan pengiraan Garisan Kelengkungan (GK) dengan menggunakan GPU dan bahagian terakhir adalah untuk melaksanakan persamaan LLE ke persamaan permukaan. Pertama, kami menggunakan Teorem Vogt dan Teorem Kneser untuk mengkaji ciri-ciri LLE dari segi monotonik. Keputusan menunjukkan bahawa LLE mempunyai ciri-ciri kelengkungan monotonik, yang memenuhi Theorem Vogt dan Theorem Kneser. Selain itu, kami menyiasat GK pada dua jenis permukaan Log Estetik (LE); Iaitu permukaan revolusi LE dan permukaan sapuan LE. Permukaan ini dijana dengan LLE yang terdiri daripada pelbagai jenis lengkung yang ditadbir oleh α. Oleh sebab GK tidak dapat diperolehi secara analitikal, kami telah melaksanakan pengiraan GK secara berangka pada CPU dan GPU yang menunjukkan kepantasan yang ketara. Di samping itu, kami menyiasat taburan kelengkungan GK dengan menggunakan Graf Kelengkungan Logarithmic. Seperti yang dijangkakan, GK pada permukaan revolusi LE sememangnya pendua lengkung profil asalnya. Walau bagaimanapun, GK pada permukaan sapuan LE adalah LLE yang berbeza bentuk kecuali kes bulatan involute, di mana jenis permukaan ini mempunyai GK dalam bentuk bulatan involutes juga. Oleh itu, GK pada permukaan LE adalah lengkung berkualiti tinggi susunan ketiga. Idea terakhir penyelidikan ini adalah menggantikan GK dengan sama ada planar atau ruang lengkung LE untuk mereka bentuk permukaan estetik baru yang dipanggil tampalan LE Coon. Dengan menggunakan paraboloid hiperbolik sebagai perbandingan, mula-mula kami memperoleh GK paraboloid hiperbolik,

menggantikannya dengan LLE dan Lengkung Ruang Log Estetik (LRLE), dan akhir sekali menjadikannya sebagai sempadan tampalan LE Coon. GK untuk kedua-dua permukaan dianalisis dengan menyiasat kelengkungan GK, terbitan kelengkungan, kilasan dan Graf Kelengkungan Logarithmic. Keputusan berangka menunjukkan bahawa kelengkungan GK untuk kedua-dua permukaan adalah monotonik manakala, profil terbitan kelengkungan bagi tampalan LE Coon adalah monotonik, tetapi bukan monotonik bagi paraboloid hiperbolik. Tambahan pula, GK pada tampalan LE Coon sememangnya LLE menunjukkan lengkung ini adalah lengkung berkualiti tinggi susunan ketiga. Oleh itu, tampalan LE Coon adalah permukaan yang berkualiti tinggi. Akhir sekali, kami mengunjurkan tampalan LE Coon kepada satah dengan menggunakan kelengkungan geodesik untuk mencipta jalur yang boleh ditampal bersama-sama sebagai tiruan proses lenturan panas dan sejuk.

SOME EXTENSIONS OF LOG AESTHETIC CURVES AND ITS ACCELERATION USING GENERAL PROCESSING UNIT (GPU)

ABSTRACT

The first part investigates the characteristics of Log Aesthetic Curve (LAC). The second part proposes new techniques to accelerate the computation of line of curvature (LoC) by using General Processing Unit (GPU) and the last part is to implement the LACs to the surface equations. We first use Vogt theorem and Kneser theorem to study the characteristics of LAC in terms of monotonicity. The results indicate that LAC has monotonic curvature characteristics, which conforms to Vogt's Theorem and Kneser's Theorem. Furthermore, we investigate the LoCs on two types of Log Aesthetic (LA) surfaces; i.e. LA surface of revolution and LA swept surfaces. These surfaces are generated with LAC which comprise of various family of curves governed by α. Since it is impossible to derive the LoCs analytically, we have implemented the LoC computation numerically on the Central Processing Unit (CPU) and GPU which showed significant speed up. Moreover, we investigated the curvature distributions of the derived LoCs using Logarithmic Curvature Graph (LCG). As expected, the LoCs on LA surface of revolutions are indeed the duplicates of its original profile curves. However, the LoCs on LA swept surface are LACs of different shapes except for the case of circle involute, where this type of surface possesses LoCs in the form of circle involutes as well. Hence, the LoCs on LA surfaces are high quality curves of order 3. The last idea on this research is to use either with planar or space Log-aesthetic curves to design a new aesthetic surface called Coon's LA patch. Using hyperbolic paraboloid as a comparison, we first derive the LoCs on hyperbolic paraboloid and approximated to LACs and LASCs, making them as the boundaries of Coon's LA patch. The LoCs for both the surfaces are analyzed by

investigating the LoC's curvature, derivative of curvature, torsion and LCG. Numerical results indicate that the LoCs for both the surfaces are monotonic curvature whereas, the derivative curvature profile of LoCs on Coon's LA patch is monotonic, but non-monotonic for hyperboloid parabolic. Furthermore, the LoCs on Coon's LA patch are indeed LACs indicating these curves are high quality curves of order 3. Hence, Coon's LA patch is a high quality surface. Lastly, we project the Coons' LA patch onto a plane using geodesic curvature to create strips which can be pasted together mimicking hot and cold bending process.

CHAPTER 1

INTRODUCTION

1.1   Background

Aesthetic curve research has been actively studied in the field of Computer Aided Geometric Design (CAGD) and Computer Aided Design (CAD). The curve can be used for the design of highways, railway route, etc. (Ahmad et al., 2007). The main characteristic of aesthetic curve is it has a monotonic curvature profile (Farin, 1996).

In 1999, Harada et al. (1999) proposed Logarithmic Distribution Diagram of Curvature (LDDC) to analyse the relationship between the length frequencies of segmented curve with regards to its radius of curvature is plotted in a log-log coordinate system. LDDC was later converted into K-vector by Kanaya et al. (2003) and eventually Logarithmic Curvature Graph (LCG) (Gobithaasan et al., 2009). In brief, the aesthetic curve has a constant gradient of LCG (Kanaya et al., 2003). Based on the features of LCG, Miura (2006) presented the linear LCG as the general formula of Log Aesthetic Curve (LAC). While curvature profile involves the second derivatives of curves, LCG involves the third derivative, hence making it suitable for higher order shape interrogation tool (Gobithaasan and Miura, 2014). The LAC family has monotonic curvature profile which can be used to represent well known spirals, e.g., clothoid, logarithmic spiral, circle involute and Nielsen's spiral. Yoshida and Saito (2006) developed a G^1 algorithm to control LAC alternatively using bisection method. Moreover, Yoshida et al. (2009) introduced Log Aesthetic Space Curve (LASC), which curvature has linear LCG and torsion has linear Logarithmic Torsion Graph (LTG). The authors also proposed a method to compute LASC segment interactively using modified Nelder and Mead's downhill simplex method. In 2009,

Levien and Sequin (2009) proved that LAC is the most promising curve for aesthetic design.

Miura et al. (2012) applied the principle of variational to the LAC and used it as digital filter. Moreover, Gobithaasan et al. (2012) introduced Generalize LASC (GLASC), an extension of LASC, adding two additional degree of freedoms into LASC. The computational time for rendering LACs can be reduced by representing LAC in the analytic form; Incomplete Gamma Function (Ziatdinov et al., 2012) or computing numerically using classical Runge-Kutta method (Gobithaasan et al, 2014a) and adaptive methods (Gobithaasan et al., 2014b). It has been shown that the classical Runge-Kutta and adaptive methods can render faster than Incomplete Gamma Function (Gobithaasan et al., 2014b) with a decent accuracy for CAD environments.

In 2012, Ziatdinov (2012) proposed a family of superspiral by generalizing LACs and developed superspiraloid by using the surface of revolution equation. Other variations of aesthetic surfaces include the work of Inoue et al. (2009) who applied LAC as profile curves to generate LA curved surface. Kineri et al. (2014) proposed LAC as a planar feature to design bi-cubic B-spline surfaces. Suzuki et al. (2018) proposed a minimum variation log-aesthetic surface as new definition of log aesthetic surface with the aid of log aesthetic filter. Recent works include developing new Log-aesthetic space curve with similarity geometry method (Miura et al., 2019), introducing τ-curve with aesthetic properties for curve generation (Miura et al., 2020) and analysing fluid flow with Log Aesthetic Curve (Wo et al., 2020).

1.2   Motivation

In 2006, Yoshida and Saito (2006) proved that LACs are drawable using drawable region. Then, Miura (2006) analysed the characteristics of LAC and

2

validated LAC has self-affinity property. However, the studies of the characteristics of LAC are countable. In 2013, Kurnosenko (2013) applied Vogt's Thoerem and Kneser's Theorem to investigate the monotonicity of Cornu spiral and biarc curve. The results indicated that these curves have monotonic curvature profiles. Hence, our first motivation is to analyse the characteristics of LAC in terms of monotonicity using Vogt's Theorem and Kneser's Theorem.

Inoue et al. (2009) developed an algorithm that used LAC as a profile curve to generate log aesthetic curved surface using VR technique. Besides that, Ziatdinov (2012) proposed a family of superspiral by generalizing LACs and developed superspiraloid by using the surface of revolution equation. In 2014, Kineri et al. (2014) designed bi-cubic B-spline surfaces by implementing LAC as a planar feature. In 2018, Suzuki et al. (2018) proposed a minimum variation log-aesthetic surface as new definition of complete LA surface using log aesthetic filter. Hence, our second motivation is to revolve a LAC about an axis that is coplanar with a circle to form LA surfaces of revolution and to sweep a LAC along another LAC to form a LA swept surface.

There are many tangent directions on a surface that can be used to generate a curve at a point which has the same surface normal direction. Hence many possible surface normal curvatures can be obtained in a particular surface normal direction. Of all the tangent directions to the point, the two tangent directions with the maximum or minimum surface normal curvature (except at umbilical and planar points) are called principal directions. In other words, the maximum or minimum surface normal curvature at that point is called the principal curvatures. A line of curvature (LoC) is a curve on a surface with tangents in the principal direction at that point.

Takezawa et al. (2016) proposed a method of using LoC to shape the doubly curved plates used in shipbuilding. There are two processes to shape the doubly curved plates. The first process is called cold bending and the next process is called hot bending. Cold bending is performed by pressing along the LoCs with smaller curvature magnitude, which causes the plate to bend along the LoC larger curvature magnitude as shown in Figure 1.1(a). Then, hot bending is applied by implementing local heat treatment along the LoC with larger curvature magnitude on the plate, causing the plate to bend along the LoC with smaller curvature magnitude as shown in Figure 1.1(b).

(a)   (b)
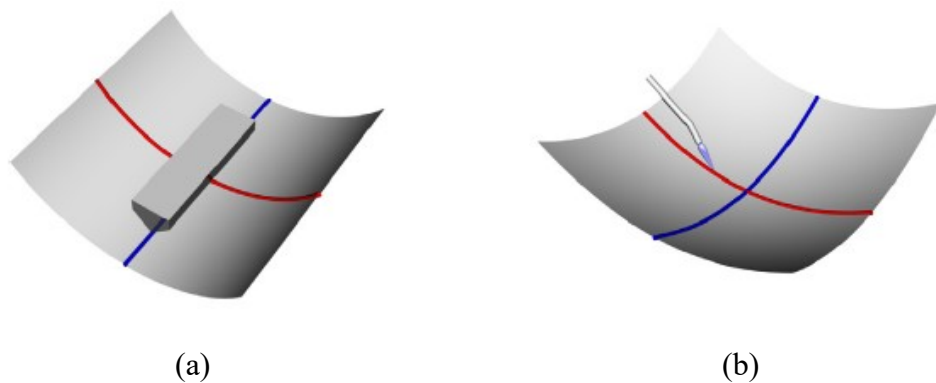
Figure 1.1   Plate bending on LoCs (Joo et al., 2014):
(a) Pressing along LoC with smaller curvature magnitude (blue line);
(b) Applying local heat treatment along LoC with larger curvature magnitude (red line).

In other words, the plates used in shipbuilding can be formed by applying these two processes to them. This indicates that LoCs molded the surface of the ship. Then, Joo et al. (2014) proposed an algorithm for computing the differential geometry properties of LoCs on parametric surfaces as well as its curvature and torsion. They further showed that these LoCs may aid in designing ship hulls. The paper also provided a way to develop LoC on a surface onto a plane using geodesic curvature.

Furthermore, Fukano et al. (2017) proposed point-based shape monitoring method for bent plates of large storage tank. The plates used to construct the storage

4

tank are similar to those used in shipbuilding industry and are very thick and difficult to bend. Note that a typical ship hull is built of 200-300 thick doubly curved plates that are more than 1cm thick (Joo et al., 2014). Fukano et al.'s (2017) method is time consuming as the process requires laser scanning to extract the desired points on the plate, identifying the differences, plate bending, and repeating the process until the desired shape is formed. Takezawa et al. (2019) proposed an interactive method to control LoCs on doubly curved surface. They smoothed the experiment surfaces by implementing smoothed directions on the LoCs instead of using true principle directions. Takezawa et al. (2021) named the patches generated by the smoothed directions as generalized principle patches. Then, they proposed a fabrication method for unfolding generalized principle patches and reconstructed them to design carbon fiber reinforced plastics automobile parts and marine propeller blades. This motivates us to analyse the relationship between LACs and LoCs on LAC surfaces such as LA surfaces of revolution and LA swept surfaces.

LoCs on typical surfaces such as hyperbolic paraboloid, elliptic paraboloid etc. can be obtained by solving an initial value problem (IVP) using numerical methods. When it comes to generating LoCs on LA surfaces, there is an additional IVP that requires to be solved numerically. The additional IVP of LAC equation itself increases the computation time for generating LoCs for LAC surfaces. One way to reduce the computation time is by means of GPUs to solve ODEs (Wolfram, 2020).

The invention GPU is intended to help gamers, researchers and programming developers enjoy their computer activities without delaying or overloading the computer. GPU performs as a labor, do a lot of repetitive works while CPU performs as an executive, master "brain" to make decision instructed by the software (Sangman et al., 2014). Parallel processing of GPUs contains large number of Arithmetic Logic

Unit's (ALU), which are better suited for dealing with repetitive work, i.e., video processing and graphical applications, than typical CPU. In addition, many researchers in various fields have implemented parallel programming for its performance in solving problems such as image processing (Yang et al., 2016), graph drawing (Qu et al., 2017) and optimization problems such as differential evolution (Qin et al., 2012) and genetic algorithms (John and Mitsuo, 2020).

Compute Unified Device Architecture or well known as CUDA is a parallel computing platform and API invented by NVIDIA for general GPUs. This technology is now readily available in various applications, including in high level scientific computation programs, e.g. Mathematica (Wo et al., 2014). There are many success stories of CUDA implementations in the field of CAD, e.g. NURBS computations (Krishnamurthy et al., 2007), moment computations (Krishnamurthy and McMains, 2011) and interactive NURBS rendering (Concheiro et al., 2014) on GPU. Hence, our fourth motivation is to implement CUDA API which is available in Mathematica to speed up the LoC's computation time in GPU.

Surface modeling is a basic mathematical method for forming surfaces in CAD application. Of all the computer-aided surface modeling methods, modeling building technique is one of the basic methods for building surfaces. There are two types of model-building techniques (Liege Universite, 2019). One is non-parametric such as subdivision surface and the other one is parametric such as NURBS surface and Coon's patch. Coon's patch is a parametric surface consisting of four curved segments connected like chains. This surface has been widely used in surface design and geometric modelling (Chang, 2015) for patching holes in a surface. NURBS surfaces are built based on control points, knots, degrees and weights (Liege Universite, 2019).

Designers can interactively compute NURBS surfaces by controlling these variables. Meanwhile, Coon's patches can be drawn by four boundary curves, which are connected like a closed fence (Chang, 2015). The advantage of Coon's patch is designers require only four boundary curves to design a surface rather than controlling each control points or weights to compute the desired surface. Examples of works include the implementation of Coon's patch for automotive design (Fan et al., 2020) and image interpolation (Qiu and Zhu, 2020). Since LoCs can be considered as edges of a surface, our motivation is to replace LoC with either planar or space Log-aesthetic curves to design a new aesthetic surface called Coon's LA patch and then analyse its LoCs. Then we can implement this technique to ship hull building.

1.3   Research Objectives

The objectives for this study are as follows:

1. To determine the basic properties of LAC using Vogt's Theorem and Kneser's Theorem,

2. To formulate LA surfaces (LA surfaces of revolution and LA swept surfaces) with various types of LACs,

3. To investigate the relationship between LACs and LoCs on LA surfaces,

4. To parallelize the evaluation of LoCs on the surface using GPUs with minimal invention of CPUs.

5. To investigate the characteristics of the Coon's patch shaped by LACs and LASCs.

1.4   Scope of Research

There are three scopes for this study.

i) Runge-Kutta methods (classical RK method and Dormand-Prince method) are used for the computation.

ii) The study will be conducted using computer software consisting of Mathematica version 11.

iii) CUDA programming runs in Mathematica by adding the functions to the string.

A computer with a specification: Intel® Core™ 2 Quad CPU Q8400 @ 2.66GHz 2.67GHz with 12GB RAM and graphic card is GeForce GT 730 with 2.0GB total memory is used to carry out the study. The computation time results may vary for different computer specifications. Figure 1.2 shows the information of computer system used to evaluate CUDA programming.

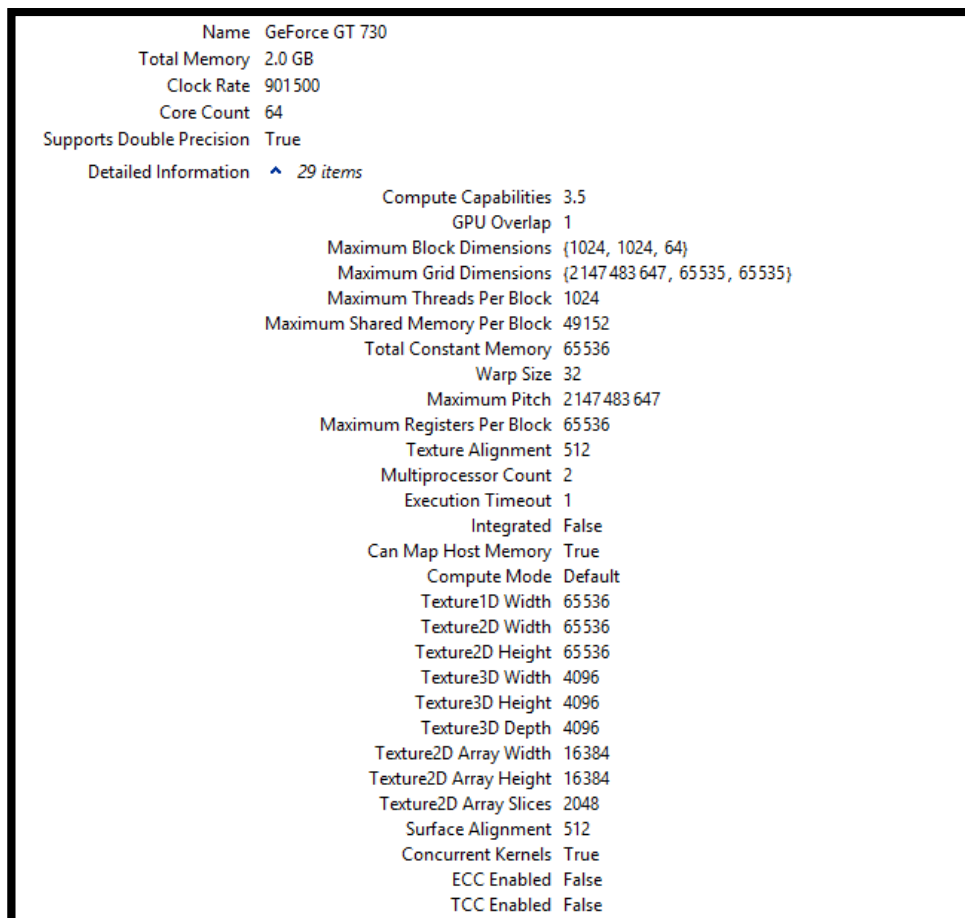|	
Name	GeForce GT 730
Total Memory	2.0 GB
Clock Rate	901 500
Core Count	64
Supports Double Precision	True
Detailed Information	⌃ 29 items
Compute Capabilities	3.5
GPU Overlap	1
Maximum Block Dimensions	{1024, 1024, 64}
Maximum Grid Dimensions	{2147 483 647, 65 535, 65 535}
Maximum Threads Per Block	1024
Maximum Shared Memory Per Block	49 152
Total Constant Memory	65 536
Warp Size	32
Maximum Pitch	2 147 483 647
Maximum Registers Per Block	65 536
Texture Alignment	512
Multiprocessor Count	2
Execution Timeout	1
Integrated	False
Can Map Host Memory	True
Compute Mode	Default
Texture1D Width	65 536
Texture2D Width	65 536
Texture2D Height	65 536
Texture3D Width	4096
Texture3D Height	4096
Texture3D Depth	4096
Texture2D Array Width	16 384
Texture2D Array Height	16 384
Texture2D Array Slices	2048
Surface Alignment	512
Concurrent Kernels	True
ECC Enabled	False
TCC Enabled	False

Figure 1.2   System information

1.5   Content of Thesis

The content of thesis consists of seven chapters specifically introduction, literature review, the characteristics of LAC, investigating the characteristics of LoCs for LA surfaces, surface design with LACs, conclusion and references.

Chapter 1 consists of background of LAC, motivation, research objectives, scopes of research, and content of thesis. Chapter 2 describes the details of LAC and LASC. Related fundamentals such as differential geometry of space curves, surfaces and curves on surface are discussed in detail. Furthermore, this chapter describes how to perform CUDA programming in Mathematica. Meanwhile, this chapter also discusses the numerical methods, Vogt's Theorem, Kneser's Theorem, surface of revolution, swept surface, Coon's patch and Bézier curve's literature review.

Chapter 3 discusses the characteristics of LAC. Vogt's Theorem and Kneser's Theorem are used to analyse the characteristics of LAC. Chapter 4 studies the formation of LA surface of revolution, LA swept surface and Quadratic Bézier swept surface. This chapter also describes the relationship between LAC and LoCs on LA surface of revolution and LA swept surface. In addition, this chapter discusses CPU and GPU performance metrics for generating LoCs.

Moreover, Chapter 5 designs Coon's LA patch and Coon's Bézier patch by applying LACs and Bézier curves as the boundaries of the surface. The curvature and torsion of LoCs are analysed and compared with hyperbolic paraboloid. The development of Coon's LA patch onto a plane is performed in this chapter. In addition, Chapter 6 discusses and concludes this research, and lastly is the references used in this research.

CHAPTER 2

LITERATURE REVIEW

2.1   Log Aesthetic Curve (LAC)

This section shows some important equations for generating LAC. The method to compute LAC interactively as shown by Yoshida and Saito (2006) is also displayed.

2.1.1   Log Aesthetic Curve Equation

In this section, Logarithmic Curvature Graph (LCG) which is the straight line (linear LCG) is used to describe about LAC equation. The LCG equation has slope, α is shown below (Yoshida and Saito, 2006):

$$\log\left(\rho\frac{ds}{d\rho}\right) = \alpha\log(\rho) + C \tag{1}$$

where s is arc-length parameterization of a curve, ρ is radius of curvature and C is constant. Using logarithmic identities, we obtain

$$\frac{ds}{d\rho} = \frac{\rho^{\alpha-1}}{\Lambda} \tag{2}$$

where $\Lambda = e^{-C}$ is parameter of LAC and $0 < \Lambda < \infty$. Integrate equation (2) then

$$s = \begin{cases} \frac{\log\rho - \log\rho_0}{\Lambda}, & \alpha = 0, \\ \frac{\rho^\alpha - \rho_0{}^\alpha}{\alpha\Lambda}, & \text{otherwise.} \end{cases} \tag{3}$$

$$\rho = \begin{cases} \rho_0 e^{\Lambda s}, & \alpha = 0, \\ (\rho_0{}^\alpha + \Lambda\alpha s)^{\frac{1}{\alpha}}, & \text{otherwise.} \end{cases} \tag{4}$$

where ρ_0 is initial radius of curvature of the curve and ρ varies from 0 to ∞. The arc-length parameterization s has upper boundary and lower boundary, depending on the

α. Table 2.1 shows the upper boundary and lower boundary of s with respect to α (Yoshida and Saito, 2006). The curvature of log aesthetic curve is shown below:

$$\kappa = \begin{cases} \dfrac{1}{\rho_0 e^{\Lambda s}}, & \alpha = 0, \\ (\rho_0{}^\alpha + \Lambda \alpha s)^{-\frac{1}{\alpha}}, & \text{otherwise.} \end{cases} \tag{5}$$

Besides that, we substitute equation (2) into $\dfrac{d\theta_T}{ds} = \dfrac{1}{\rho}$ (Yoshida and Saito, 2006):

$$\frac{d\theta_T}{ds}\frac{ds}{d\rho} = \frac{d\theta_T}{d\rho} = \frac{1}{\rho}\frac{\rho^{\alpha-1}}{\Lambda} = \frac{\rho^{\alpha-2}}{\Lambda}. \tag{6}$$

Integrate equation (6) then we have

$$\rho = \begin{cases} \rho_0 e^{\Lambda\theta_T}, & \alpha = 1, \\ (\rho_0{}^{\alpha-1} + \Lambda(\alpha-1)\theta_T)^{\frac{1}{\alpha-1}}, & \text{otherwise.} \end{cases} \tag{7}$$

The boundaries of θ_T (the angle between the tangent vectors of the given two endpoints) are shown in Table 2.1.

Table 2.1   The upper boundary and lower boundary of s and $\boldsymbol{\theta_T}$ (Yoshida and Saito, 2006)

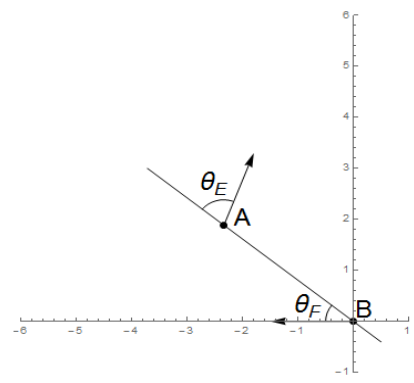| s			$\boldsymbol{\theta_T}$		
α	Lower Bound	Upper Bound	α	Lower Bound	Upper Bound
$\alpha < 0$	-	$-\dfrac{\rho_0{}^\alpha}{\alpha\Lambda}$	$\alpha < 1$	-	$\dfrac{\rho_0{}^{\alpha-1}}{(1-\alpha)\Lambda}$
$\alpha = 0$	-	-	$\alpha = 1$	-	-
$\alpha > 0$	$-\dfrac{\rho_0{}^\alpha}{\alpha\Lambda}$	-	$\alpha > 1$	$\dfrac{\rho_0{}^{\alpha-1}}{(1-\alpha)\Lambda}$	-

To note, we can draw LAC by applying equation (5) to the Frenet-Serret formula and set torsion equals to 0.

2.1.2 Interactive Log Aesthetic Curve Segment

Yoshida and Saito (2006) implemented a method to compute LAC interactively with given two endpoints and their tangent direction. Table 2.2 shows how LAC is computed using the given two endpoints and their tangent direction.

Table 2.2   Computing LAC interactively

Step	Description	Graph
1	Determine θ_E and θ_F of endpoints A and B. θ_E and θ_F can be obtained by calculating the angle from tangent vector to the chord AB and $\theta_T = \theta_E + \theta_F$.	
2	With $\theta_E > \theta_F$, the original points with its tangent direction are transformed using translation, rotation and reflection with condition: a) If $\alpha > 1$, point A is at origin {0,0} and its tangent direction is on x-axis (unit tangent vector of A is {1,0}),	
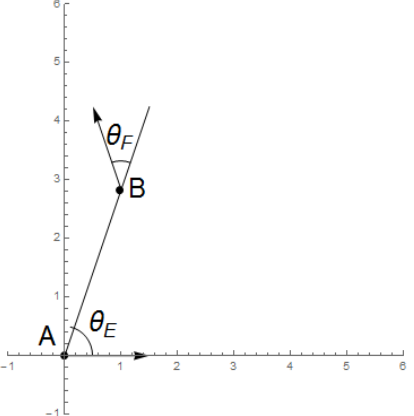
	b) If $\alpha \leq 1$, point B is at origin $\{0,0\}$ and its tangent direction is on x-axis (unit tangent vector of B is $\{-1,0\}$).	
3	Use bisection method to get s and Λ value that satisfies given G^1 data with the calculated θ_T values.	
4	Generate LAC segment (color red) with calculated θ_T and Λ values and the endpoint at θ_T is labelled as point C. (Assuming $\alpha = -1$)	
5	Calculate the length from point B to point C and from point B to point A and then compute the ratio. The ratio will be the scaling factor for the curve segment.	
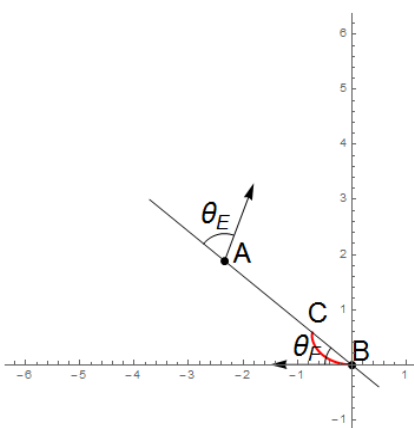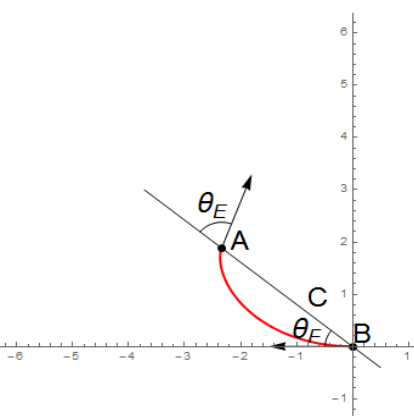
6	Inverse transformations are performed until the two endpoints of the curve segment return to the original position of points A and B.	

2.2 Log Aesthetic Space Curve (LASC)

Log Aesthetic Space Curve is an extension of LAC. In 2009, Yoshida et al. (2009) proposed that the setting of Logarithmic Torsion Graph (LTG) is similar to LCG and can be used to generate space curves. To note, the torsion of LAC is 0. Yoshida et al. (2009) introduced that LASC is a curve whose curvature and torsion are either monotonic increasing or monotonic decreasing. Hence, the torsion of the curve is similar to curvature of the curve. Based on equation (5), the torsion of LASC can be defined as below:

$$\tau = \begin{cases} \dfrac{1}{\mu_0 e^{\Omega s}}, & \beta = 0, \\ \left(\mu_0{}^\beta + \Omega\beta s\right)^{-\frac{1}{\beta}}, & \text{otherwise.} \end{cases} \tag{8}$$

where τ is torsion of curve, μ_0 is initial radius of torsion (Yoshida et al., (2009) assumed this as a parameter), Ω is a shape parameter, β is the slope of LTG and s is the arc-length of curve. If the curve is rendered from 0 to $-$s, then its torsion is monotonic increasing and vice-versa. Table 2.3 shows the upper boundary and lower boundary of s with respect to β.
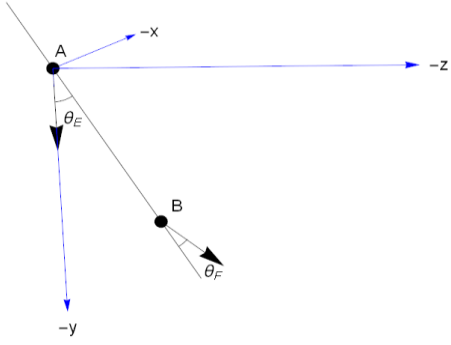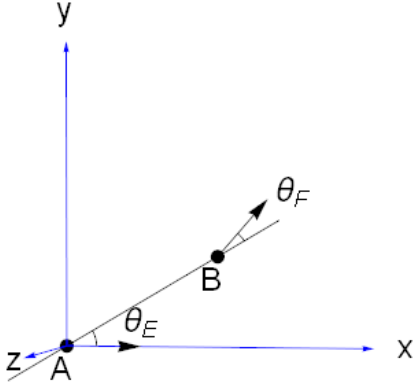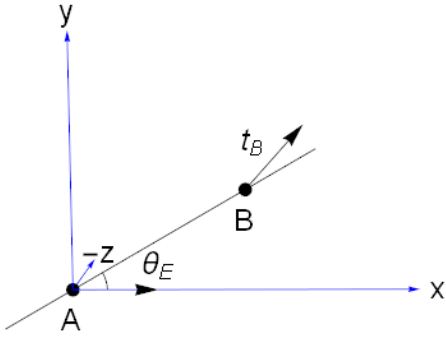
14

Table 2.3   The upper boundary and lower boundary of *s*

β	Lower Bound of *s*	Upper Bound of *s*
$\beta < 0$	-	$-\dfrac{\mu_0{}^\beta}{\beta\Omega}$
$\beta = 0$	-	-
$\beta > 0$	$-\dfrac{\mu_0{}^\beta}{\beta\Omega}$	-

The boundaries of s are varied depend on the combination of the curve's curvature and torsion as stated in Yoshida et al. (2009) paper. This paper proposed a method to compute LASC interactively as shown in Table 2.4. The method is similar to the method used to compute LAC. Note that we use Frenet-Serret formula to generate LASC numerically. The initial value of the unit tangent, normal and binormal vector are set as $t(0) = \{1,0,0\}$, $n(0) = \{0,1,0\}$ and $b(0) = \{0,0,1\}$. When we rotate the endpoint about x-axis to the xy plane, the sign of z-coordinate of $t(s)$ is negative.

Table 2.4   Drawing LASC interactively

Step	Description	Graph
1	Determine θ_E and θ_F of two endpoints A and B from the given G^1 data. θ_E and θ_F can be obtained by calculating the angle from tangent vector to the chord AB and $\theta_E > \theta_F$.	

2	Move points A and B until point A is at origin {0,0,0}.	
3	Rotate point B and tangent vector of points A and B about the point {0,0,0} until tangent vector of point A is on the x-axis. Then, rotate point B and its tangent vector about x-axis until point B is on the xy-plane.	
4	If the sign of z-coordinate of point B's tangent vector (t_B) is positive, the z-coordinate of point B's tangent vector is reversed. All z-coordinates of the points on the curve segment are reversed.	
5	Generates the LASC segment from endpoint C (at origin) to endpoint D and then rotates the segment and endpoint's tangent vector (t_D) until endpoint D is on the xy-plane. Set the parameters Ω and ρ_0, and then use bisection method to find the arc-length, s of LASC that satisfies $\theta_D = \theta_E$. Then, use Nelder and Mead's	

16
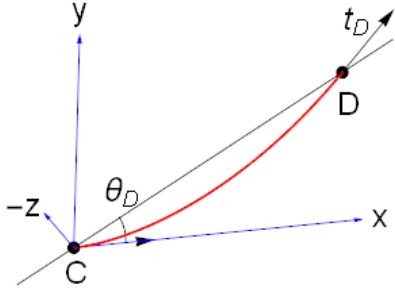
	downhill simplex method to find parameters Λ and μ_0 that satisfy $t_B.t_D = 1$. Repeat Step 5 until both conditions are met.	
6	Scale the LASC segment until its endpoints are at points A and B.	
7	If Step 4 occurs, all z-coordinates of the points on the curve segment are reversed. Inverse transformations are performed until the two endpoints of the curve segment return to the original position of points A and B.	

This is why Step 4 is necessary. Nelder and Mead's downhill simplex method is a simplex method to find local minimum for several variables (Quinten, 2013). In our case, there are two variables (Λ and μ_0) are required to minimize $f(\Lambda, \mu_0) = |t_B.t_D - 1| = 0$. The simplex method of two variables requires three simplex points (x_1, x_2 and x_3 where $x = \{\Lambda, \mu_0\}$) that move like amoeba to approach to the minimum value of the function. First, function $f(\Lambda, \mu_0)$ is evaluated on each of the three simplex points to find the best point ($\boldsymbol{B}$), second best point ($\boldsymbol{S}$) and worst point ($\boldsymbol{W}$) from the three simplex points. Then, the midpoint $\boldsymbol{M} = \frac{\boldsymbol{B+S}}{2}$ is calculated. Next, calculate the reflection point $\boldsymbol{R}$, Expansion point $\boldsymbol{E}$ and Contraction point $\boldsymbol{C}$ where $\boldsymbol{R} = \boldsymbol{M} +$

$(\boldsymbol{M} - \boldsymbol{W})$, $\boldsymbol{E} = \boldsymbol{M} + 2(\boldsymbol{R} - \boldsymbol{M})$ and $\boldsymbol{C} = \boldsymbol{M} + 0.5(\boldsymbol{M} - \boldsymbol{W})$. The original paper (Quinten, 2013) included one more step is to shrink the triangle (from three simplex points) to smaller triangle. We found that it took more time to minimise the function. Hence, we removed this step from the entire minimization. Figure 2.1 shows the flowchart of the Nelder and Mead downhill simplex algorithm.
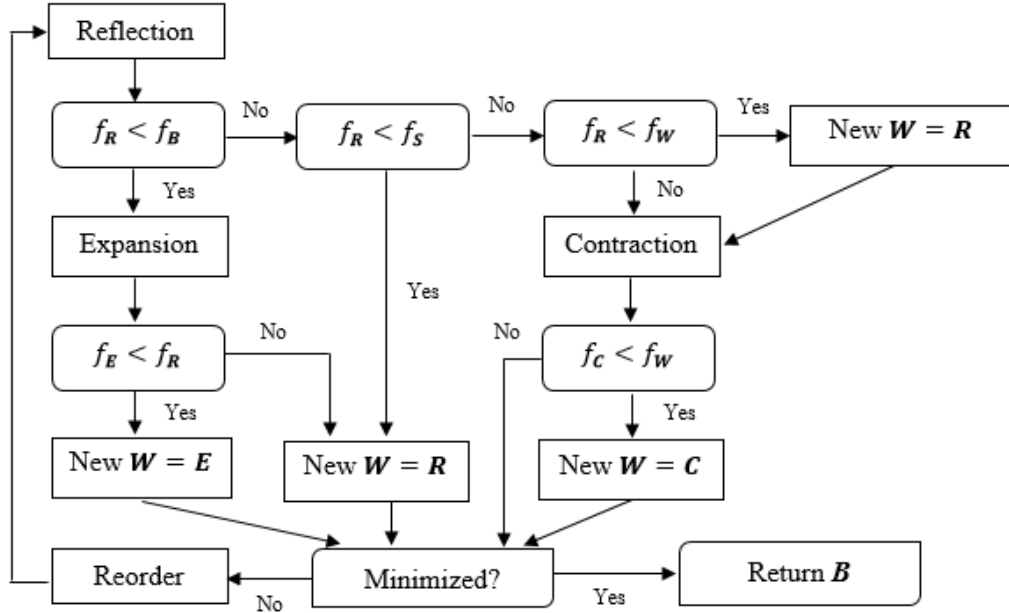

Figure 2.1 Nelder and Mead's downhill simplex algorithm

2.3   Space Curve

Frenet-Serret Formulas in term of arc-length parameterization, s are (Marsh, 2005):

$$\boldsymbol{t}'(s) = \kappa(s)\boldsymbol{n}(s),$$

$$\boldsymbol{n}'(s) = -\kappa(s)\boldsymbol{t}(s) + \tau(s)\boldsymbol{b}(s),$$

$$\boldsymbol{b}'(s) = -\tau(s)\boldsymbol{n}(s),$$

(9)

where $\boldsymbol{t}$ is tangent vector, $\boldsymbol{n}$ is normal vector and $\boldsymbol{b}$ is binormal vector of the curve. Let $\boldsymbol{C}(s)$ be a parametric curve, we have : (Joo et al., 2014)

18

$$C(s) = \{x(s), y(s), z(s)\}, \tag{10}$$

$$C'(s) = t(s), \tag{11}$$

$$C''(s) = t'(s) = \kappa(s)n(s), \tag{12}$$

$$C'''(s) = \kappa'(s)n(s) + \kappa(s)n'(s). \tag{13}$$

In addition, assuming that $\varphi(u) = \frac{ds}{du}$ and then the Frenet-Serret formulas in terms of parameter u are defined as the following (Marsh, 2005):

$$\dot{t}(u) = \frac{dt(u)}{du} = \varphi(u)\kappa(u)n(u),$$

$$\dot{n}(u) = \frac{dn(u)}{du} = \varphi(u)\big(-\kappa(u)t(u) + \tau(u)b(u)\big), \tag{14}$$

$$\dot{b}(u) = \frac{db(u)}{du} = -\varphi(u)\tau(u)n(u).$$

2.4 Vogt's Theorem

Vogt's theorem is a theorem used to analyse the existence of a spiral from a given turning angle, which is rarely used to extend well-known curves. In 1914, Vogt's Theorem was introduced to analyse convex arcs of planar curves with constant sign monotonic curvature (Kurnosenko, 2013). Then Guggenheimer (1977) reformulated Vogt's Theorem as follows:

"Let A and B be the endpoints of a spiral arc, the curvature nondecreasing from A to B. The angle θ_B of the tangent to the arc at B with the chord AB is not less than the angle θ_A of the tangent at A with AB. $\theta_A = \theta_B$ only if the curvature is constant."

Kurnosenko (2013) studied the existence and positional inequality of short spirals and long spirals, necessary and sufficient conditions of it using Vogt's Theorem. The

results show that as long as the curve has monotonic curvature profile, it is credible. Kurnosenko (2013) modified Vogt's Theorem as follows:

Vogt's Theorem (Short Spirals): The boundary angles θ_A and θ_B of a normalized short spiral or circular arc satisfy the conditions below:

$$
\begin{aligned}
&if\ \kappa_1 < \kappa_2: & \theta_A + \theta_B > 0, && -\pi < \theta_A \leq \pi, && -\pi < \theta_B \leq \pi; \\
&if\ \kappa_1 > \kappa_2: & \theta_A + \theta_B < 0, && -\pi \leq \theta_A < \pi, && -\pi \leq \theta_B < \pi; \\
&if\ \kappa_1 = \kappa_2: & \theta_A + \theta_B = 0, && -\pi < \theta_A < \pi, && -\pi < \theta_B < \pi.
\end{aligned}
\tag{15}
$$

The author defined the meaning of short spiral and normalized spiral. Short spiral indicates that a planar curve with monotonic continuous curvature is short if it does not intersect the complement of its chord to the infinite straight line. Besides that, a normalized spiral or arc is an arc that is scaled and transformed so that its starting point is located at position A (coordinate $\{-c, 0\}$ on the x-axis) and the endpoint is located at position B (coordinate $\{c, 0\}$ on the x-axis). The best solution is to equal c to 1 so that the product $c\kappa(s) \equiv \kappa(s)$ will be called as normalized curvature and the arc becomes a normalized dimensionless quantity.
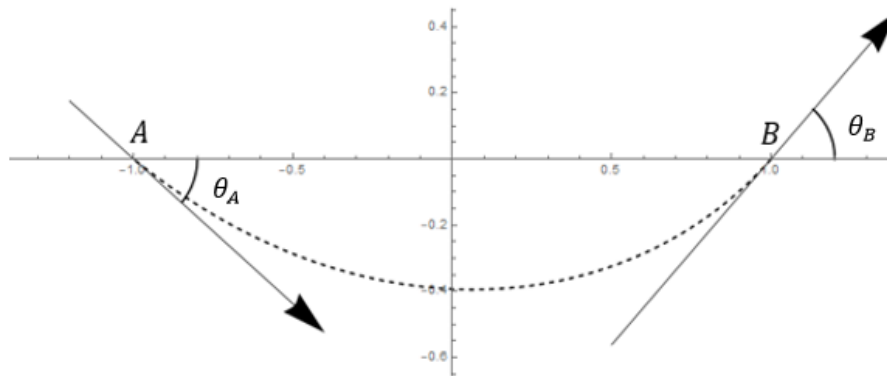

Figure 2.2 Normalized short arc

Figure 2.2 shows the image of a normalized short spiral. It is important to note that when a curve is rendered from one end to the other and the curvature's sign is the same

sign, the curve is a C-Spiral. Also, if the curvature of both endpoints are of different signs, then the curve is an S-Spiral. In other words, the curve is rendered from positive to negative curvature (or vice-versa) to form an S-Spiral. Since LAC has its limitations and extra constraints, our objective dwells around this theorem to prove the monotonicity of LAC for given input.

2.5   Kneser's Theorem

Kneser's Theorem analysed the properties of spiral using circle of curvature method (Guggenheimer, 1977). In the absence of inflection points, the author defined Kneser's Theorem on a spiral as follows:

"Any circle of curvature of a spiral arc contains every smaller circle of curvature of the arc in its interior and in its turn is contained in the interior of every circle of curvature of greater radius."
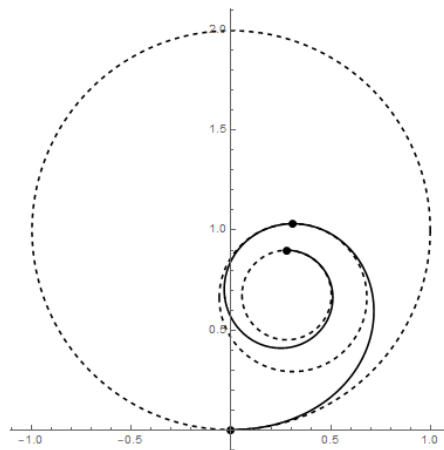

Figure 2.3 Spiral and its circles of curvature

Figure 2.3 shows the idea of Kneser's Theorem. To note, the dashed circles are circles of curvature of different points on the spiral. The curvature of the circle of curvature is based on the curvature of the spiral at that point. If the smaller circle of curvature is contained in a larger circle of curvature, then the spiral satisfies Kneser's Theorem.

2.6   Surface

The first fundamental equation of the surface is (Patrikalakis and Maekawa, 2001):

$$I(u, v) = ds^2 = E\,du^2 + 2F\,du\,dv + G\,dv^2$$

where $E = \boldsymbol{R}_u \cdot \boldsymbol{R}_u$, $F = \boldsymbol{R}_u \cdot \boldsymbol{R}_v$, $G = \boldsymbol{R}_v \cdot \boldsymbol{R}_v$ and $\boldsymbol{R} = \boldsymbol{R}(u, v)$ is a parametric surface. The function of first fundamental equation is to calculate the arc-length and the surface area. The arc-length of curve on a surface and surface area can be calculated using equations below:

$$\text{ArcLength} = \int_{t_0}^{t_1} \sqrt{E\dot{u}^2 + 2F\dot{u}\dot{v} + G\dot{v}^2}\,dt, \tag{16}$$

$$\text{Surface Area} = \int_{v_0}^{v_1} \int_{u_0}^{v_1} \sqrt{EG - F^2}\,du\,dv, \tag{17}$$

where $\dot{\boldsymbol{u}} = \dfrac{du}{dt}$ and $\dot{\boldsymbol{v}} = \dfrac{dv}{dt}$.

Example 1 (Patrikalakis and Maekawa, 2001)

Let's take hyperbolic paraboloid as an example:

$$\text{Hyperbolic Paraboloid} = \boldsymbol{R}(u, v) = \{u, v, uv\} \tag{18}$$

$$E = 1 + v^2, F = uv, G = 1 + u^2.$$

Assume that the parametric curve on the surface of hyperbolic paraboloid, $\boldsymbol{C}$ is given:

$$\boldsymbol{C}\big(u(t), v(t)\big) = \{t, t\},$$

$$\dot{u}(t) = \frac{du}{dt} = 1, \dot{v}(t) = \frac{dv}{dt} = 1.$$

With $0 \le t \le 1$, we can further compute the arc-length of the curve:

$$\text{ArcLength} = \int_0^1 \sqrt{(1+t^2)(1)^2 + 2(t)(t)(1)(1) + (1+t^2)(1)^2} \, dt$$

$$= \int_0^1 \sqrt{2+4t^2} \, dt$$

$$= \frac{1}{2}\left(\sqrt{6} + \sinh^{-1}\sqrt{2}\right) = \sqrt{\frac{3}{2}} + \frac{1}{2}\log(\sqrt{2}+\sqrt{3}) \approx 1.79785.$$

To calculate the surface area of hyperbolic paraboloid, the boundaries of parameters u and v must be given. The area of hyperbolic paraboloid equation is shown below:

$$\text{Surface Area} = \int_{v_0}^{v_1} \int_{u_0}^{u_1} \sqrt{(1+u^2)(1+v^2) - (uv)^2} \, du \, dv.$$

Suppose that $u = r\cos\theta$, $v = r\sin\theta$, $0 \le r \le 1$ and $0 \le \theta \le \frac{\pi}{2}$, then:

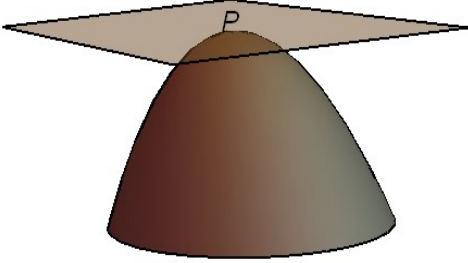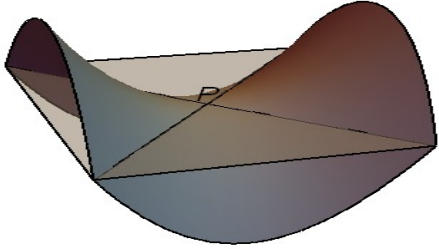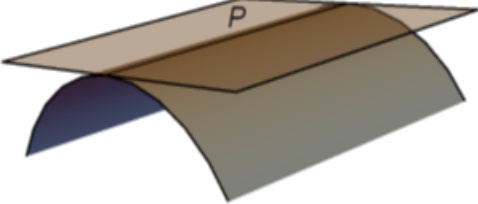$$\text{Surface Area} = \int_0^1 \int_0^{\frac{\pi}{2}} r\sqrt{(1+r^2)} \, d\theta \, dr = \frac{\pi}{6}\left(-1 + 2\sqrt{2}\right).$$

Next, the second fundamental equation is: (Patrikalakis and Maekawa, 2001)

$$\text{II}(u,v) = L \, du^2 + 2M \, du \, dv + N \, dv^2$$

where $L = \mathbf{N} \cdot \boldsymbol{R}_{uu}$, $M = \mathbf{N} \cdot \boldsymbol{R}_{uv}$ and $N = \mathbf{N} \cdot \boldsymbol{R}_{vv}$ and $\mathbf{N} = \frac{R_u \times R_v}{|R_u \times R_v|}$ is the unit normal vector of the surface point. The second fundamental equation can be used to investigate the shape of a surface. There are four common cases can be determined using second fundamental equation as shown in Table 2.5 (Patrikalakis and Maekawa, 2001). The plane on the surface is the tangent plane at point P. K and H indicate Gaussian and mean curvatures which their formulas are given.

The first case is the elliptic point on the surface, Point P is the only point touches its tangent plane, and the normal curvatures at point P are all at the same sign. In the second case, the tangent plane cut through and divides the points on the surface

Table 2.5   Relationship between surface shape and second fundamental equation

Case	Description	Graph
Elliptic point	$LN-M^2 > 0$ $(K > 0)$ and $H \neq 0$	
Hyperbolic point	$LN-M^2 < 0$ $(K < 0)$ and $H \neq 0$	
Parabolic point	$LN-M^2 = 0$ $(K = 0)$, $L^2+N^2+M^2 \neq 0$ and $H \neq 0$	
Planar point	$L = M = N = 0$	

into two sides. Hence, point P is the hyperbolic point. In other words, the sign of normal curvature at point P can be positive or negative depending on the tangent direction at that point. Furthermore, point P in the third case is a parabolic point that produces a line of intersection between paraboloid and tangent plane. The occurrence of line of intersection is caused by zero normal curvature on the paraboloid surface. The last case is the planar point at which the tangent plane is parallel to the planar